Subcritical Dissipation in Three-Dimensional Superflows

C. Nore,[1] C. Huepe,[2] and M. E. Brachet[2]
[1]Université Paris XI, Laboratoire d'Informatique pour la Mécanique et les Sciences de l'Ingénieur, CNRS, BP 133, 91403 Orsay cedex, France
[2]Laboratoire de Physique Statistique de l'Ecole Normale Supérieure, associé au CNRS et aux Universités Paris 6 et 7, 24 Rue Lhomond, 75231 Paris Cedex 05, France
(Received 29 November 1999)

Three-dimensional (3D) superflows past a circular cylinder are studied by numerically integrating the nonlinear Schrödinger equation. 3D initial data are built from the two-dimensional (2D) stationary vortex nucleation solutions. Quasistationary half-ring vortices, pinned at the sides of the cylinder, are generated after a short time. On a longer time scale, either 3D vortex stretching induces dissipation and drag, or the vortex is absorbed by the cylinder. The corresponding 3D critical velocity is found to be well below the 2D one. The implications for experiments in Bose-Einstein condensed gas and low-temperature helium are discussed.

PACS numbers: 67.40.Hf, 03.75.Fi, 67.40.Vs

Dilute Bose-Einstein condensates have been recently produced experimentally [1]. The dynamics of these compressible nonlinear quantum fluids is accurately described by the nonlinear Schrödinger equation (NLSE), also called the Gross-Pitaevskii equation [2], allowing direct quantitative comparison between theory and experiment [3]. The NLSE can also be considered to describe the dynamics of superfluid ^{4}He, at temperatures low enough for the normal fluid to be negligible. In the homogeneous two-dimensional (2D) NLSE flow past a disk, Frisch *et al.* [4] found the existence of a transition to dissipation due to the periodic emission of pairs of counterrotating vortices. This transition was shown to occur at a critical Mach number $M_{2\mathrm{D}}^c$ always greater than 0.35 [5]. Vortex formation and pressure drag above $M_{2\mathrm{D}}^c$ were extensively studied [6]. In a recent experiment, Raman *et al.* have studied dissipation in a Bose-Einstein condensed gas by moving a blue detuned laser beam through the condensate at different velocities [7]. In their inhomogeneous condensate, they observed a critical Mach number for the onset of dissipation $M_{2\mathrm{D}}^c/1.6$.

The main problem addressed in this Letter is the characterization of an intrinsically three-dimensional (3D) vortex stretching mechanism in the superflow around a cylinder. Such a mechanism is made plausible by recent 3D NLSE simulations and experiments in ^{4}He [8] demonstrating the existence of vortex stretching and inertial range Kolmogorov scaling in superfluid turbulence. This 3D mechanism generates drag and can be responsible for the subcritical (below $M_{2\mathrm{D}}^c$) dissipation observed by Raman *et al.* [7].

We study the effect of a moving cylinder of diameter D in a 3D superfluid at rest described by the action

$$\mathcal{A} = \int dt \left\{ \sqrt{2}\, c\xi \int d^3x\, \frac{i}{2}\left(\bar\psi \frac{\partial \psi}{\partial t} - \psi \frac{\partial \bar\psi}{\partial t}\right) - \mathcal{F} \right\}, \tag{1}$$

where ψ is a complex field and $\bar\psi$ is its conjugate. The coherence length ξ and the speed of sound c (for a mean fluid density $\rho_0 = 1$) are the physical parameters characterizing the superfluid. The energy $\mathcal{F}$ reads

$$\mathcal{F} = \mathcal{E} - \vec{\mathcal{P}} \cdot \vec{U}, \tag{2}$$

where

$$\mathcal{E} = c^2 \int d^3x \Big([-1 + V(\vec{x})]\,|\psi|^2 + \frac{1}{2}\,|\psi|^4 + \xi^2 |\nabla\psi|^2 \Big)$$

and

$$\vec{\mathcal{P}} = \sqrt{2}\, c\xi \int d^3x\, \frac{i}{2}\,(\psi\nabla\bar\psi - \bar\psi\nabla\psi) \tag{3}$$

is the superfluid momentum. The repulsive potential $V(r) = (V_o/2)\{\tanh[4(r - D/2)/\ell] - 1\}$ represents the cylinder, whose velocity $\vec{U}$ is imposed by the $\vec{\mathcal{P}} \cdot \vec{U}$ term. In the calculations presented below, $V_o = 10$ and $\ell = \xi$. With these values, the field inside the cylinder is negligible ($|\psi| \sim 0$) and the boundary layer is well resolved with a mesh adapted to the coherence length.

The NLSE is the Euler-Lagrange equation corresponding to (1),

$$\frac{\partial\psi}{\partial t} = i\,\frac{c}{\sqrt{2}\,\xi}\,[\Omega(\vec{x})\psi - |\psi|^2\psi + \xi^2\nabla^2\psi] + \vec{U}\cdot\nabla\psi, \tag{4}$$

where $\Omega(\vec{x}) = 1 - V(|\vec{x}|)$.

The NLSE (4) can be mapped into two hydrodynamic equations by applying Madelung's transformation: $\psi = \sqrt{\rho}\exp(i\phi/\sqrt{2}\,c\xi)$, where ρ and $\vec{v} = \nabla\phi - \vec{U}$ are the fluid density and velocity relative to the cylinder. We thus obtain the continuity equation $\partial\rho/\partial t + \nabla\cdot(\rho\vec{v}) = 0$ and the Bernoulli equation $\partial\phi/\partial t + \vec{v}^{\,2}/2 - \vec{U}^2/2 + c^2[\rho - \Omega(\vec{x})] - c^2\xi^2\nabla^2\sqrt{\rho}/\sqrt{\rho} = 0$. The last term of this equation is a dispersive supplementary "quantum pressure" term that is relevant only at length scales smaller than ξ. Note that the NLSE (4) admits vortical solutions of characteristic core size $\sim\xi$. These are topological defects (zeros) of the complex field ψ and thus appear as points in 2D and lines in 3D.

In our previous studies [5], the bifurcation diagram of stationary solutions to the NLSE describing a 2D superflow around a disk were obtained using Fourier pseudospectral methods and continuation techniques. In Fig. 1, the energy (2) of the stationary solutions is presented as a function of the Mach number $M = |\vec{U}|/c$ for different values of ξ/D. The stable ($0V$) and unstable symmetric ($2V$) and asymmetric ($1V$) branches are connected through a primary saddle node and a secondary pitchfork bifurcation. While $0V$ corresponds to a laminar flow, $1V$ and $2V$ display one and two vortices, respectively, near the sides of the cylinder. The corresponding dynamics was studied by numerical integrations of the NLSE (4). Beyond the saddle-node critical Mach number $M_{2\mathrm{D}}^c$, no stationary solution exists and (dissipative) periodic vortex nucleation occurs. No subcritical dissipation was observed in this 2D system. The value of $M_{2\mathrm{D}}^c$ was found to depend on ξ/D, with a lower bound at $M_{2\mathrm{D}}^c \sim 0.35$, reached in the limit $\xi/D \to 0$ [5].

We used the 2D laminar stationary solution $\psi_{0V}(x,y)$ (corresponding to branch $0V$) and the one-vortex unstable stationary solution $\psi_{1V}(x,y)$ (branch $1V$) to construct the 3D initial condition $\psi_{3\mathrm{D}}(x,y,z) = f_{\mathrm{I}}(z)\psi_{1V}(x,y) + [1 - f_{\mathrm{I}}(z)]\psi_{0V}(x,y)$. The function $f_{\mathrm{I}}(z)$, defined by $f_{\mathrm{I}}(z) = \{\tanh[(z - z_1)/\Delta_z] - \tanh[(z - z_2)/\Delta_z]\}/2$, takes the value 1 for $z_1 \le z \le z_2$ and 0 elsewhere (Δ_z is an adaptation length). The surface $|\psi_{3\mathrm{D}}| = 0.5$ is shown in Fig. 2a, for $\xi/D = 0.025$, $|\vec{U}|/c = 0.26$, and $\Delta_z = 2\sqrt{2}\,\xi$ in the $[L_x \times L_y \times L_z]$ periodicity box ($L_x/D = 2.4\sqrt{2}\,\pi$, $L_y/D = 1.2\sqrt{2}\,\pi$, and $L_z/D = 0.4\sqrt{2}\,\pi$). The cylinder surface and the initial condition vortex line, with both ends pinned to the left side of the cylinder, are apparent in the figure.

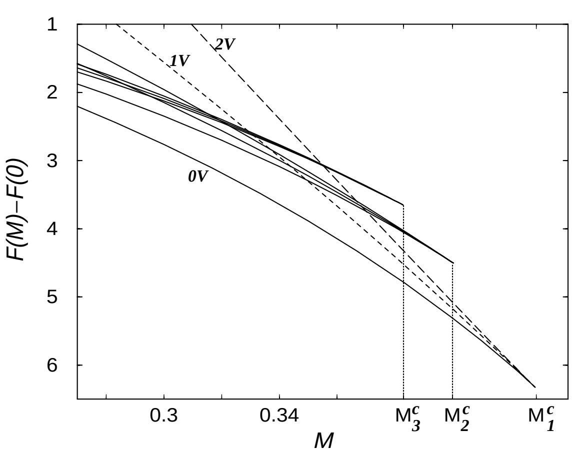

FIG. 1. Plot of the energy of the stationary solutions [$\mathcal{F}(M) - \mathcal{F}(0)$, per unit vertical length] versus Mach number ($M = |\vec{U}|/c$) for $\xi/D = 1/10,\ 1/20,\ 1/40$. Stable branch: solid line ($0V$). Unstable asymmetric branch: dashed line ($1V$). Unstable symmetric branch: long-dashed line ($2V$). The saddle-node bifurcation is marked by M_i^c, with $M_1^c(1/10) = 0.429$, $M_2^c(1/20) = 0.4$, and $M_3^c(1/40) = 0.383$.

The resulting dynamical evolution is obtained by integrating the NLSE, with a 3D version of the code used in our previous studies [5]. It can be schematically described in terms of short-time and long-time dynamics.

Under short-time dynamics, the initial pinned vortex line rapidly contracts, evolving through a decreasing number of half-ring-like loops, down to a single quasistationary half ring (see Figs. 2b–2d). If the initial vortex line is long enough to contract to quasistationary half rings, the evolution always takes place near the plane perpendicular to the flow. If the vortex line is too small, it moves upstream and collapses against the cylinder.

The diameter d of a stationary vortex ring in an infinite Eulerian flow with no obstacle is given by [9]

$$|\vec{U}|/c = (\sqrt{2}\,\xi/d)[\ln(4d/\xi) - K], \tag{5}$$

where $|\vec{U}|$ is the flow velocity at infinity and the vortex core model constant $K \sim 1$ is obtained by fitting the numerical results in [10]. This equation can be used to check that the half-ring state (Fig. 2d) is quasistationary. Indeed, the local flow velocity v in a low-Mach number Eulerian flow around a cylindrical obstacle varies from $v = |\vec{U}|$ at infinity to $v = 2|\vec{U}|$ at both sides of its surface. For the values used in Fig. 2, local velocities therefore range from $v = 0.25$ to $v = 2 \times 0.25$. Equation (5) implies that

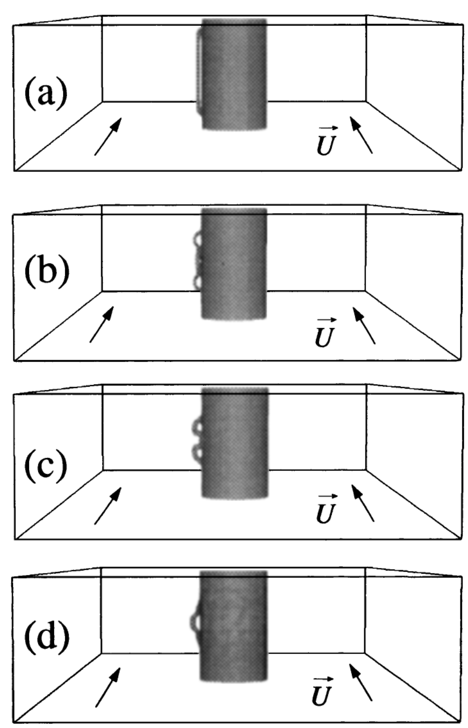

FIG. 2. Short-time dynamics of a vortex pinned to the cylinder for run 6 (see Table I below). The surface $|\psi| = 0.5$ is shown at times (a) $t = 0$, (b) $t = 40\sqrt{2}\,\xi/c$, (c) $t = 60\sqrt{2}\,\xi/c$, and (d) $t = 80\sqrt{2}\,\xi/c$. Note that the half ring formed on (d) has the diameter needed to be approximately stationary [see text below Eq. (5)].

TABLE I. General characteristics of all runs. The horizontal periodicity lengths are $L_x/D = 2.4\sqrt{2}\,\pi$ and $L_y/D = 1.2\sqrt{2}\,\pi$. The adimensional drag coefficient C_x is indicated when vortex stretching takes place (NS: no stretching), except for run 6 [see text below Eq. (7)].

Run	M	ΔM	$t_{\rm end}c/\xi$	ξ/D	L_z/D	C_x
1	0.30	7%	$300\sqrt{2}$	0.05	$0.8\sqrt{2}\,\pi$	1.0
2	0.35	9%	$250\sqrt{2}$	0.05	$2.4\sqrt{2}\,\pi$	0.5
3	0.22	9%	$250\sqrt{2}$	0.04	$0.8\sqrt{2}\,\pi$	0.4
4	0.25	4%	$625\sqrt{2}$	0.04	$0.8\sqrt{2}\,\pi$	0.9
5	0.25	12%	$225\sqrt{2}$	0.033	$0.8\sqrt{2}\,\pi$	0.6
6	0.26	23%	$300\sqrt{2}$	0.025	$0.4\sqrt{2}\,\pi$	*
7	0.35	9%	$50\sqrt{2}$	0.1	$0.8\sqrt{2}\,\pi$	NS
8	0.30	7%	$150\sqrt{2}$	0.067	$0.8\sqrt{2}\,\pi$	NS
9	0.37	0%	$75\sqrt{2}$	0.067	$0.8\sqrt{2}\,\pi$	NS
10	0.25	4%	$150\sqrt{2}$	0.05	$0.8\sqrt{2}\,\pi$	NS
11	0.15	20%	$150\sqrt{2}$	0.033	$0.8\sqrt{2}\,\pi$	NS

the diameter of a stationary half ring should be bounded by $d(v = 0.25) = 18.8\xi$ and $d(v = 2 \times 0.25) = 6.3\xi$. The diameter $d \approx 9\xi$ measured on the half ring observed in Fig. 2d is thus consistent with its quasistationary behavior. The diameter of the half ring shown below in Fig. 3 (inset), $d \approx 7.6\xi$, is similarly found to be between the corresponding bounds $d(0.35) = 11.4\xi$ and $d(2 \times 0.35) = 3\xi$.

On a longer time scale, the quasistationary half ring can evolve in two opposite ways: it starts moving either upstream or downstream. When the half ring is driven downstream, the vortex loop is continuously stretched while the pinning points move towards the back of the cylinder. When the half ring moves upstream, it eventually collapses against the cylinder, generating a laminar superflow. In order to distinguish between the two situations we have carried out 3D runs summarized in Table I. Most runs were performed at Mach numbers M slightly different from that of the 2D stationary solutions $M_{\rm 2D}$. The value of $\Delta M = (M - M_{\rm 2D})/M$ is indicated in the table. These 3D computations are rather expensive, e.g., to integrate the NLSE up to the situation in Fig. 3b (run 2) necessitates a resolution of $256 \times 128 \times 256$ and 25 hours of CPU on a Cray 90 machine.

Figure 3 shows the long-time dynamics for a stretching case: run 2 of Table I. The inset in Fig. 3b pictures the corresponding quasistationary half ring for size comparison. Note that, as the vortex loop grows, its rear part remains oblique to the flow (see Fig. 3a).

The runs of Table I are displayed schematically in Fig. 4. The runs with vortex stretching are labeled by circles and those without by $\times$. All runs were performed at Mach numbers below $M_{\rm 2D}^c(\xi/D)$, indicated in Fig. 4 as a solid line. The experimental [7] critical Mach number and value of ξ/D are marked by an asterisk.

For $1/30 < \xi/D < 1/20$, there is a frontier between the dissipative and nondissipative cases that can be drawn approximately as the dashed line in Fig. 4, which corresponds to the expression $R_s = 5.5$ with

$$R_s \equiv |\vec{U}|D/c\xi = MD/\xi\,. \tag{6}$$

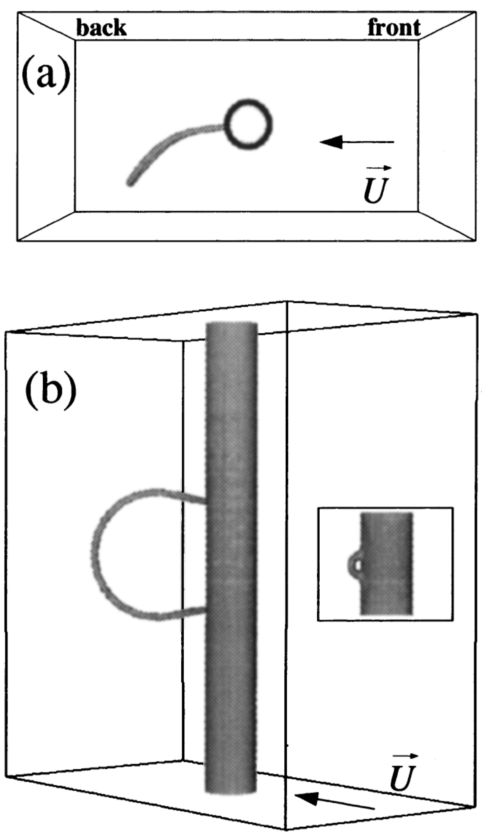

FIG. 3. Top (a) and side (b) views of the stretched vortex pinned to the cylinder at the end of run 2 (see Table I). The inset shows the corresponding quasistationary half-ring solution obtained at $t = 40\sqrt{2}\,\xi/c$.

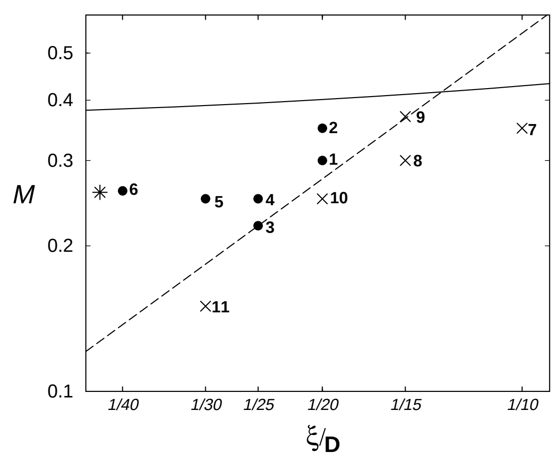

FIG. 4. Parametric study of vortex stretching in a Mach number M versus ξ/D log-log diagram. Circles: stretching; crosses: no stretching (labels are run numbers of Table I). The asterisk represents the experiment reported in [7]. The solid line is the 2D saddle-node bifurcation Mach number $M_{\rm 2D}^c$ as a function of ξ/D and the dashed line represents Eq. (6) (see text).

This superfluid "Reynolds" number is defined in the same way as the standard (viscous) Reynolds number $\mathrm{Re} \equiv |\vec{U}|D/\nu$ (with ν the kinematic viscosity). In the superfluid turbulent ($R_s \gg 1$) regime, R_s was shown to be equivalent to the standard (viscous) Reynolds number Re [8]. Note that, for a Bose condensate of particles of mass m, the quantum of velocity circulation around a vortex, $\Gamma = 2\pi\sqrt{2}\,c\xi$, has the Onsager-Feynman value $\Gamma = h/m$ (h is Planck's constant) and the same physical dimensions L^2T^{-1} as ν.

In order to study quantitatively the transition to dissipation, we define the nondimensional drag

$$C_x = 2(d|\vec{\mathcal{P}}|/dt)/\rho_0|\vec{U}|^2 S\,, \tag{7}$$

where the surface S facing the flow is the diameter D of the cylinder times the height of the vortex loop obtained at the end of the run. Typically, the superfluid momentum (3) as a function of time (data not shown) first oscillates during the short-time dynamics. In the case of vortex stretching it then grows linearly. In this case, $d\vec{\mathcal{P}}/dt$ is estimated by a linear fit to $\vec{\mathcal{P}}$. The case of run 6 is special. Although vortex stretching took place, it was impossible to reliably determine C_x because the height of the vortex loop kept on growing during the run. This may be due to the lower value of L_z/D in this run. The values of C_x are displayed in Table I. The obtained order-one values of C_x demonstrate that 3D vortex stretching is an efficient dissipative mechanism.

In our numerical system, the initial vortex loop was imposed extrinsically. In an experimental setting, fluctuations strong enough to nucleate the initial vortex loop are needed to commence vortex stretching. The vortex nucleation by thermal or quantum fluctuations has been studied by different groups [11,12]. Ihas *et al.* proposed a nucleation barrier formed by an unstable stationary vortex loop that is pinned to the walls bounding the superflow. Interestingly, this solution is equivalent to the quasistationary half-ring solution towards which our numerical system is driven naturally before starting vortex stretching.

In summary, our numerical results demonstrate the possibility of a subcritical (below $M^c_{2\mathrm{D}}$) and efficient ($C_x \sim 1$) drag mechanism, based on 3D vortex stretching. Our computations were performed for values of ξ/D comparable to those in Bose-Einstein condensed gas experiments [7]. In the context of superfluid ^{4}He flow, the experimental critical velocity is known to depend strongly on the system's characteristic size D. It is often found to be well below the Landau value (based on the velocity of roton excitation) except for experiments where ions are dragged in liquid helium. Feynman's alternative critical velocity criterion $R_s \sim \log(D/\xi)$ is based on the energy needed to form vortex lines. It produces better estimates for various experimental settings but does not describe the vortex nucleation mechanism [9]. It would be very interesting to determine experimentally the dependence of the critical Mach number on the parameter ξ/D and the nature (2D or 3D) of the excitations.

We acknowledge useful scientific discussions with V. Hakim, L. Tuckerman, and E. Varoquaux. This work was supported by ECOS-CONICYT Program No. C96E01. Computations were performed at the Institut du Développement et des Ressources en Informatique Scientifique.

[1] M. H. Anderson, J. R. Ensher, M. R. Matthews, C. E. Wieman, and E. A. Cornell, Science **269**, 198 (1995); K. B. Davis, M. O. Mewes, M. R. Andrews, N. J. van Druten, D. S. Durfee, D. M. Kurn, and W. Ketterle, Phys. Rev. Lett. **75**, 3969 (1995); C. C. Bradley, C. A. Sackett, and R. G. Hulet, Phys. Rev. Lett. **78**, 985 (1997).

[2] E. P. Gross, Nuovo Cimento **20**, 454 (1961); L. P. Pitaevskii, Sov. Phys. JETP **13**, 451 (1961).

[3] F. Dalfovo, S. Giorgini, L. P. Pitaevskii, and S. Stringari, Rev. Mod. Phys. **71**, 463 (1999).

[4] T. Frisch, Y. Pomeau, and S. Rica, Phys. Rev. Lett. **69**, 1644 (1992).

[5] C. Huepe and M. E. Brachet, C. R. Acad. Sci. Paris **325**, 195 (1997); C. Huepe and M. E. Brachet, Physica D (Amsterdam) (to be published).

[6] B. Jackson, J. F. McCann, and C. S. Adams, Phys. Rev. Lett. **80**, 3903 (1998); T. Winiecki, J. F. McCann, and C. S. Adams, Phys. Rev. Lett. **82**, 5186 (1999).

[7] C. Raman, M. Köhl, R. Onofrio, D. S. Durfee, C. E. Kuklewicz, Z. Hadzibabic, and W. Ketterle, Phys. Rev. Lett. **83**, 2502 (1999).

[8] C. Nore, M. Abid, and M. E. Brachet, Phys. Rev. Lett. **78**, 3896 (1997); C. Nore, M. Abid, and M. E. Brachet, Phys. Fluids **9**, 2644 (1997); M. Abid, M. E. Brachet, J. Maurer, C. Nore, and P. Tabeling, Eur. J. Mech. B, Fluids **17**, No. 4, 665 (1998).

[9] R. J. Donnelly, *Quantized Vortices in Helium II* (Cambridge University Press, Cambridge, England, 1991).

[10] C. A. Jones and P. H. Roberts, J. Phys. A **15**, 2599 (1982).

[11] C. M. Muirhead, W. F. Vinen, and R. J. Donnelly, Proc. R. Soc. London A **402**, 225 (1985).

[12] G. G. Ihas, O. Avenel, R. Aarts, R. Salmelin, and E. Varoquaux, Phys. Rev. Lett. **69**, 327 (1992).